Ideal-Observer Based Metric for MR Image Quality Assessment - Application to Lesion Detection

C. G. Graff[1], and K. J. Myers[1]
[1]Division of Imaging and Applied Mathematics, U. S. Food and Drug Administration, Silver Spring, MD, United States

Objectives: New MR sequences and reconstruction algorithms necessitate image quality (IQ) metrics. Traditionally SNR, CNR or MSE are used, however they do not take into account the imaging task. MR images are used to provide information about the patient to the radiologist; thus it is logical to base the IQ metric on the ability of a reader to perform a clinical task. This is known as objective assessment of image quality (OAIQ) [1] which is used in the evaluation of other modalities but has not yet been developed for MR. The objective of this work is to present initial work on OAIQ metrics for MR, in this case the Ideal Observer SNR for lesion detection.

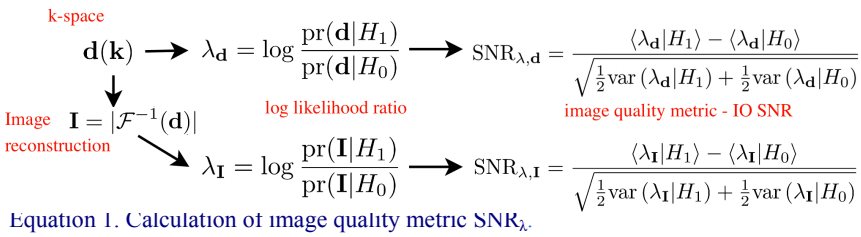

Equation 1. Calculation of image quality metric SNR_λ.

Methods: Consider the task of determining if a patient *P* has a lesion (hypothesis H_1) or does not (hypothesis H_0). The patient is imaged, resulting in k-space data ***d(k)*** which is reconstructed to produce image ***I(r)***. Typically the observer who reads the image is a human, but here we employ the Ideal (Bayesian) Observer (IO) which serves as an upper-bound on human performance. The IO can act on the data or reconstructed images, thus we consider 2 observers, each of which calculate a log-likelihood ratio λ for *P* and compares it to a threshold λ_{th} to decide H_1 or H_0. The random variable λ is the logarithm of the ratio of the probability distribution of the k-space data (or reconstructed image) conditioned on the two hypotheses. The IQ metric is the IO signal-to-noise ratio SNR_λ, calculated as the difference in the expected value of λ conditioned on the two hypotheses divided by the averaged standard deviation. The relationship between the data and SNR_λ is summarized in Eq. 1. Equation 2 gives the probability distributions required for λ. The data follows a Gaussian noise distribution with data point $d_{j,c}$ having mean value $\mu_{j,c|Hk}$ given hypothesis H_k, *k=0* or *1*. Variable *j* indexes k-space location and *c* indexes coil in a multi-coil acquisition. The pixels in a sum-of-squares inverse FFT reconstruction follow a non-central chi distribution [2] where I_{C-1} is the modified Bessel function of order *C-1* and $\nu_{j|Hk}$ is the mean pixel value conditioned on H_k.

$$\mathrm{pr}(\mathbf{d}|H_k) = \prod_{j,c=1}^{J,C} \frac{1}{\sqrt{2\pi\sigma}} \exp\left(-\left(\mu_{j,c|H_k} - d_{j,c}\right)^2 / 2\sigma^2\right)$$

$$\mathrm{pr}(\mathbf{I}|H_k) = \prod_{j=1}^{J} \frac{\nu_{j|H_k}}{\sigma_i^2} \exp\left(-\left(\nu_{j|H_k}^2 + I_j^2\right)^2 / 2\sigma_i^2\right) \left(\frac{I_j}{\nu_j}\right)^C I_{C-1}\left(\frac{I_j \nu_{j|H_k}}{\sigma_i^2}\right)$$

Equation 2. Probability distributions of the k-space data and image pixels.

$$\mathrm{SNR}_{\lambda,\mathbf{d}} \propto \mathrm{SNR} \cdot r_l \sqrt{\sum_j \left|e^{-t_j/T2_l^*} - e^{-t_j T2_b^*}\right|^2 \frac{|J_1(2\pi r_l |\mathbf{k}_j|)|^2}{|\mathbf{k}_j|^2}}$$

Equation 3. Relationship between $\mathrm{SNR}_{\lambda,\mathbf{d}}$, traditional SNR, contrast and k-space acquisition strategy.

Results: To illustrate the SNR_λ calculation, consider the detection of a circular lesion of radius r_l with relaxation time $T2^*_l$ embedded in a homogeneous background object with relaxation time $T2^*_b$ using a standard echo-planar acquisition. Equation 3 shows that $\mathrm{SNR}_{\lambda,\mathbf{d}}$ is proportional to traditional SNR, but also incorporates information about lesion size (r_l), contrast (differences in $T2^*$ between background and lesion) and which k-space locations k_p are sampled (at time t_p). J_1 is a first order Bessel function which appears in the k-space representation of a circular lesion. Figure 2 is a contrast-detail diagram for $\mathrm{SNR}_{\lambda,\mathbf{d}}$ showing how T2* contrast and lesion size effect SNR_λ. Figure 3 compares SNR_λ for different lesion sizes and number of coils showing a difference between $\mathrm{SNR}_{\lambda,\mathbf{d}}$ and $\mathrm{SNR}_{\lambda,\mathbf{I}}$ for higher numbers of coils, caused by the non-optimality of sum-of-squares reconstructions [3] which leads to information loss in the reconstruction process.

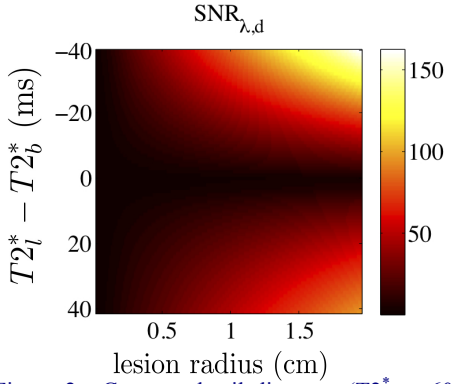

Figure 2: Contrast-detail diagram. ($T2^*_b$ = 60 ms, FOV = 24 cm, matrix 64x64, BW = ±32 kHz, SNR = 20, single coil acquisition)

Conclusion: We have shown how OAIQ can be applied to MR imaging by evaluating a simple lesion detection task. The results demonstrate that the ability to detect a lesion is not fully characterized by traditional SNR metrics. This framework can be extended to more complex tasks, objects and imaging system models to provide clinically-relevant measures of the effectiveness of new acquisitions and reconstruction techniques.

References: [1] Barrett, H.H. and Myers, K.J., *Foundations of Image Science*, Wiley & Sons (2004). [2] Dietrich, O. et al., Magn Reson Imaging **26**:754-762 (2008) [3] Larsson, E.G., et al., J Magn Reson **163**:121-123 (2003).

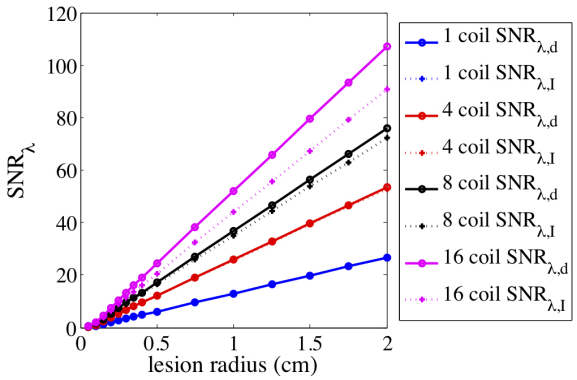

Figure 3: SNR_λ vs. lesion size. ($T2^*_b$ = 30 ms, $T2^*_l$ = 60 ms, FOV = 24 cm, 64x64 matrix, BW = ±32 kHz, SNR = 20)